Measurement of the Thermal Conductivity Anisotropy in Polyimide Films

Katsuo Kurabayashi, *Member, IEEE*, Mehdi Asheghi, Maxat Touzelbaev, and Kenneth E. Goodson, *Associate Member, IEEE*

***Abstract*— Polymer films are playing an important role in the development of micromachined sensors and actuators, fast logic circuits, and organic optoelectronic devices. The thermal properties of polyimide films govern the temporal response of many micromachined thermomechanical actuators, such as ciliary arrays. This work develops three experimental techniques for measuring both the in-plane and the out-of-plane thermal conductivities of spin-coated polyimide films with thicknesses between 0.5 and 2.5 μm, which are common in MEMS. Two of the techniques use transient electrical heating and thermometry in micromachined structures to isolate the in-plane and out-of-plane components. These techniques establish confidence in a third, simpler technique, which measures both components independently and uses IC-compatible processing. The data illustrate the anisotropy in the thermal conductivity of the polyimide films investigated here, with the in-plane conductivity larger by a factor between four and eight depending on film thickness and temperature. The anisotropy diminishes the time constants of thermal actuators made from polyimide films. [375]**

***Index Terms*— Anisotropy, electrical resistance thermometry, Joule heating, polyimide films, thermal conductivity.**

I. Introduction

POLYMER films of thickness near 1 μm are playing an important role in the development of micromachined sensors, actuators, logic circuits, and organic optoelectronic devices. The high thermal expansion coefficients of polymers make them particularly attractive for use in micromachined thermal actuators including V-groove joints [1] and ciliary arrays [2]. The temporal responses of these actuators are strongly influenced by the thermal conduction properties of the polymer films. Polymer layers are being developed for application as low-dielectric-constant passivation for multilevel metallization in highly integrated circuits [3]–[5]. The lower dielectric constant diminishes the electrical signal delay along the interconnect, which is a critical bottleneck for the development of faster logic circuits. Electrically conducting polymer films are being developed for organic layers in optoelectronic devices because of the ease with which they can be processed, their low cost, and their high electroluminescence efficiency [6]. For application as active and passive layers in circuitry, the low thermal conductivities of polymers yield very large temperature rises and temperature gradient magnitudes in metallization and devices. This will augment electromigration-induced interconnect failure and reduce the lifetime of organic devices.

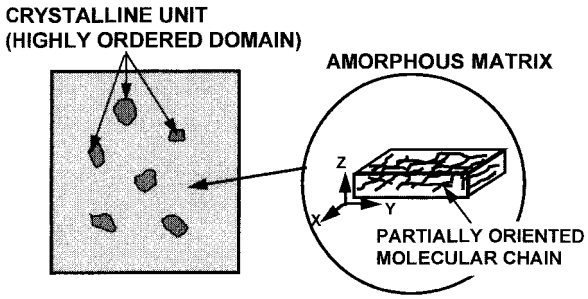

Fig. 1. Schematic of the microstructure of semicrystalline polyimide. The spin-coating process leads to alignment in the plane of the film for both the crystalline and the noncrystalline phases.

The properties of polymer layers can be anisotropic and depend strongly on the details of the process by which they are made. Previous studies illustrated the anisotropy in the index of refraction [7], [8] and the dielectric constant [9] of these layers. The Young's modulus and the thermal expansion coefficient depend on the molecular stoichiometry, the fraction of the material which is crystalline, as well as the length and orientation of the molecular chains, all of which vary with processing details and the layer thickness [10]–[12]. This makes the use of bulk data inappropriate for the simulation of the thermomechanical behavior of microfabricated structures containing organic thin films. Anisotropy and a similar disparity between bulk and thin-film properties are expected to prevail for the thermal conductivity. Using transient grating methods, Rogers *et al.* [13] measured the in-plane thermal diffusivities of polymer films with thicknesses between 1 and 9 μm. Their results indicate that the thermal conduction properties of these films may differ from those of bulk polymer materials due to the anisotropy of the thin films.

Fig. 1 approximately depicts the microstructure of semicrystalline polyimide films, which contain crystalline domains dispersed in an amorphous matrix. Anisotropy in the thermal and mechanical properties can result from the anisotropy of the crystalline domains. Another mechanism responsible for the anisotropy is the ordering of the crystalline domains or of the molecular chains in the surrounding matrix. Choy *et al.* [14]

Manuscript received August 6, 1998; revised February 23, 1999. This work was supported by the Semiconductor Research Corporation under Contracts 98-PJ-357 and 98-SJ-461. The work of K. E. Goodson was supported by the Office of Naval Research through the Young Investigator Program and the National Science Foundation through a CAREER Award. Subject Editor, E. Obermeier

The authors are with the Department of Mechanical Engineering, Stanford University, Stanford, CA 94305-3030 USA.

Publisher Item Identifier S 1057-7157(99)04267-5.

calculated the effective thermal conductivities along $(k_{c//})$ and perpendicular $(k_{c\perp})$ to molecular chains of a polyethylene crystal for the case in which the chains are perfectly parallel with one another. These authors predicted a large value of the thermal conductivity anisotropy, $k_{c//}/k_{c\perp} > 10^3$. Morelli *et al.* [15] measured the thermal conductivities of single-crystal diacetylenes parallel and perpendicular to the chain direction at low temperature and observed thermal conductivity anisotropy of $k_{c//}/k_{c\perp} \approx 60$. The weak Van der Waals interaction between the neighboring chains impedes the transport of atomic vibrational energy and leads to a relatively large thermal resistance for conduction between the chains. The strong coupling of atomic vibrations along the chains enhances energy transport and yields more effective thermal transport in that direction. Ho *et al.* [10] observed that the amorphous matrix has a high degree of molecular orientation in the film plane. The partial alignment of the polymer molecular chains can result from the spin-on process used in deposition of polymer interlayer dielectric films on a silicon substrate. The polyimide films studied in the present work are expected to have a very small volume fraction of the crystalline phase. Therefore, if the thermal conductivity anisotropy can be observed in these films, it is mainly due to the partial alignment of polymer chains in the amorphous structure.

Thermal properties of dielectric films have been investigated using a variety of different measurement techniques [16], [17]. Several steady-state techniques measured the thermal conductivity of dielectric and semiconducting thin films using Joule heating and electrical-resistance thermometry in patterned metal bridges [18]–[20]. The thermal conductivity is extracted from a solution to the heat-diffusion equation considering the applied heating power, the geometry of the measurement structure, and the measured temperature rises in the two bridges. Using this approach in suspended membrane structures, Völklein and Kessler [21] measured the thermal conductivities of bismuth layers of thicknesses between 200 and 4000 Å. Transient techniques have also been developed to measure thermal conductivity and diffusivity of dielectric thin films. One approach monitors the time-dependent temperature rise in a metallic layer deposited on a dielectric film following a brief heating pulse. To induce the short pulsed heating and monitor the temperature of the sample surface, Okuda *et al.* [22] applied pulsed current to a metal interconnect and measured the time evolution of its electrical resistance. Käding *et al.* [23] used a short laser pulse for heating and measured the reflectivity change of the metal coating. Another approach is to apply a harmonic current to a metal bridge deposited on the film surface and to use the third harmonic of the voltage response for measuring the resulting temperature oscillation magnitude. This approach has been used extensively at frequencies below 10 kHz for measurements of the effective vertical thermal conductivity of disordered layers [24]–[27]. Ju *et al.* [28] used a similar approach at frequencies up to 100 kHz by combining harmonic electrical heating with laser-reflectance thermometry. These studies either neglected lateral conduction in the dielectric layers or assumed that the thermal conductivity is isotropic. Although this approach is well suited for extracting the vertical conductivity, it is not appropriate for measuring the lateral thermal conductivity in anisotropic materials including the polymers studied here.

Several experimental techniques have been used for studying anisotropic thermal conduction in uniaxially stretched bulk polymers. Kilian *et al.* [29] and Blum *et al.* [30] measured the thermal conductivities parallel and perpendicular to the deformation direction of polyethylene slabs. Their method generated an instantaneous heating region at the center of the sample surface using either a hot needle or a focused laser beam. The isotherms on the sample surface were imaged using a liquid crystal coating. The shape of the isotherms was an ellipse, which had major and minor axes parallel and perpendicular to the deformation direction, respectively. The ratio of the lengths of the principal axes was used to calculate the thermal conductivity anisotropy factor of the polymer slab. An alternative technique was recently developed by Rantala [31] for measuring the anisotropy ratio of uniaxially stretched polymer foils. The method of Rantala [31] places a steady-state heating wire on the sample surface and detects temperatures at several points from the wire to a direction perpendicular to it using an infrared detector. Independent measurements were performed for two experimental samples, each of which had a heating wire placed either along or perpendicular to the deformation direction. The detected temperature profile yields data for the thermal conductivity anisotropy. These methods are well suited for studying thermal conductivity anisotropy of bulk solids subjected to controlled stress.

There is a need for a method that examines the thermal conductivity anisotropy in films of thickness near 1 μm, for which the spin-on process can yield strong anisotropy between the in-plane and out-of-plane directions. This work develops three independent techniques for measuring the vertical and lateral thermal conductivities of polymer films. One of the techniques uses free-standing polymer membranes to capture the lateral thermal conductivity, while a second technique uses extensive ion etching to form a mesa structure that isolates the vertical conductivity. While these techniques reduce the experimental uncertainty by isolating components of the conductivity tensor, they are difficult to implement on a broad variety of samples due to the extensive micromachining. This problem motivates the development of a technique that applies to polymer layers on silicon, also described in this manuscript, which is based on samples that are made entirely with conventional IC fabrication technology. The IC compatible technique is the most practical approach for the on-chip characterization of a wide variety of novel organic passivation layers. The data obtained using the IC compatible method are compared with those from the other two independent techniques.

II. Mesa Vertical Conductivity Method

This section describes an experimental structure and procedure which measures the vertical conductivity of polymer films. The data are obtained using steady-state Joule heating and electrical-resistance thermometry in two metal bridges. Kleiner *et al.* [20] used this approach for measuring the thermal conductivities for conduction normal to SiO_2 layers. They performed the measurements using a structure with

two parallel metal bridges embedded in SiO_2 passivation. Their arrangement results in experimental errors due to heat spreading from the edges of the top bridge to the surrounding passivation layer, which reduces the heat flux reaching the second bridge. The present work designs an experimental structure such that the measurements can be performed without the source of these errors and extracts the data with a small experimental uncertainty.

A. Micromesa Structure Fabrication

Fig. 2 shows the experimental structure used for measuring the vertical thermal conductivity of polymer films in the current study. The structure in Fig. 2 uses a mesa geometry, which restricts heat conduction in the direction normal to the film. The resulting data are therefore influenced only by the effective vertical conductivity. The fabrication of the mesa structure is summarized in Fig. 3. First, a silicon dioxide layer of thickness near 3000 Å is grown on a 4-in silicon wafer using thermal oxidation. Second, a 2500-Å film of aluminum is sputtered onto the silicon dioxide and patterned using chemical wet etching. The silicon wafer is spin-coated with an organic adhesion-promoter of thickness comparable to 100 Å. Third, a layer of polyamic acid precursor (Du Pont PI 2556: benzophenone tetracarboxylic dianhydride 4, 4-oxydianiline m-phenylene diamine, BTDA-ODA-MPD) is spin-coated onto the wafer. The thickness of the polymer precursor is varied between 0.5 and 2.1 μm by changing the rotational frequency of the spinner. The polyamic acid films are cured in a nitrogen atmosphere by heating from room temperature to 375 °C at the rate of 7 °C per minute followed by 1 h at 375 °C. The samples are allowed to cool in room-temperature air. Fourth, a silicon nitride layer of thickness near 1000 Å is deposited using plasma-enhanced CVD (PECVD). The silicon nitride prevents the polymer films from absorbing moisture during the processing and enhances adhesion of the metallization deposited subsequently. Finally, an overlaying aluminum layer (~2500 Å) is deposited on the PECVD silicon nitride layer using sputtering and is patterned using wet etching. The mesa structure is achieved using plasma etching of the polymer with the aluminum serving as a mask. The thickness of the polymer is measured using profilometry, optical interferometry, and a cross-sectional scanning electron micrograph, all of which yield values differing by less than 2%. The thickness of the silicon nitride and the metal layers are measured using profilometry and cross section electron microscopy.

B. Experimental Procedure

The structure depicted in Fig. 2 provides electrical-resistance thermometers directly above and below the dielectric layer under investigation. This eliminates the need for analysis of heat conduction in the underlying substrate and strongly reduces the contribution of the temperature rise in the substrate to the uncertainty in the data. The electrical resistances of the aluminum bridges are calibrated as functions of temperature using a heated chuck at a probe station. A relatively large dc current (>0.3 A) is applied to the top

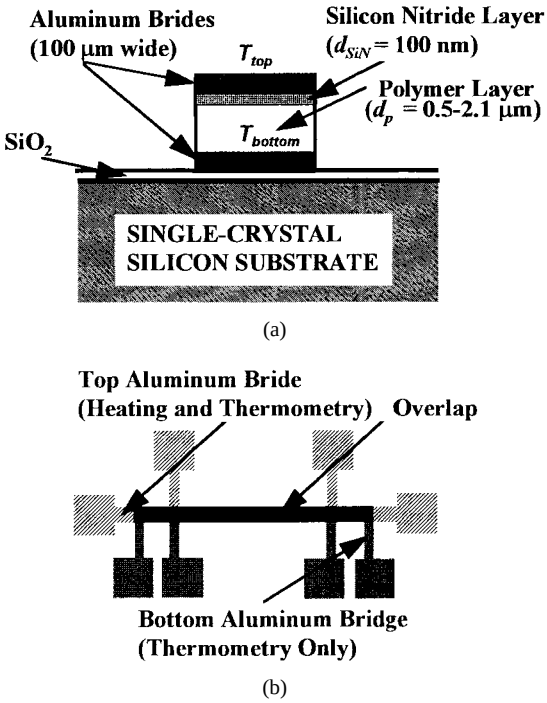

Fig. 2. (a) Cross-sectional and (b) top-view schematics of the micromesa structure used for measurement of the vertical thermal conductivity.

heating/thermometry line to yield a temperature rise near 10 K. The current applied to the bottom thermometry bridge is chosen such that the temperature rise and heating power are both negligible compared to those in the overlying bridge. Heat loss to the ambient air at the top and sides of the mesa structure are negligible. The steady-state temperature rises of the two bridges resulting from the Joule heating of the top bridge are extracted from their electrical resistance change, which is determined through simultaneous four-point measurements of current and voltage.

The temperature difference between the top and the bottom bridges is $T_{\rm top}-T_{\rm bottom}$ and the heat flux density generated at the top line is q'', which is the ratio of the total electrical power and the area of the heating line. The total thermal resistance of the silicon-nitride/polymer two-layer system, $R_{\rm total}$, is extracted using

$$R_{\rm total}=\frac{T_{\rm top}-T_{\rm bottom}}{q''}=\frac{d_p}{k_{pn}}+\frac{d_{\rm SiN}}{k_{\rm SiN}}+R_b \qquad (1)$$

where d_p, $d_{\rm SiN}$, k_{pn}, $k_{\rm SiN}$, and R_b are the polymer thickness, the silicon-nitride thickness, the intrinsic thermal conductivity vertical to the polymer layer, the intrinsic thermal conductivity vertical to the silicon nitride layer, and the sum of the thermal resistances at the aluminum/silicon-nitride, silicon-nitride/polymer, and polymer/aluminum interfaces. The silicon-nitride thickness $d_{\rm SiN}$ is 1000 Å. The thermal conductivity of a silicon nitride layer fabricated using the same processing conditions is measured independently, in the absence of the underlying polymer, using a three-bridge method documented previously [19]. The thermal conductivity of the silicon nitride obtained using the three-bridge method is 0.8 W K^{-1} m^{-1}, which agrees within the experimental uncertainty with the value reported by previous authors for silicon nitride

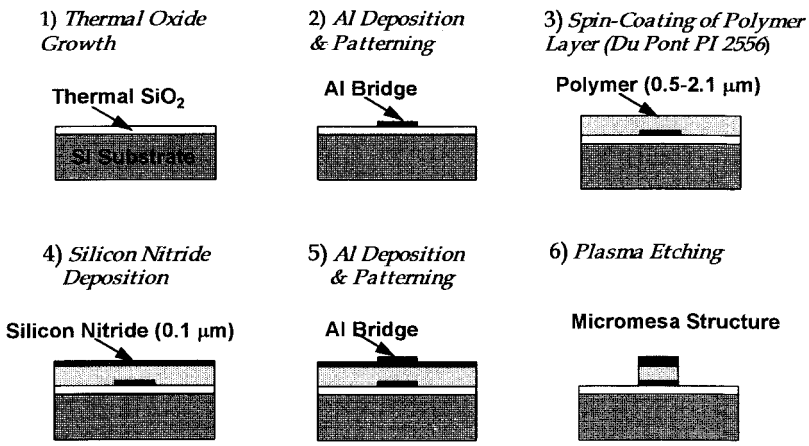

Fig. 3. Microfabrication steps for the structure in Fig. 2.

layers of thickness near 1000 Å [27]. Based on the data for the nitride layer, it is possible to extract the thermal resistance resulting from the polymer volume and the boundaries R_p

$$R_p = R_{\text{total}} - \frac{d_{\text{SiN}}}{k_{\text{SiN}}} = \frac{d_p}{k_{pn}} + R_b. \tag{2}$$

The relative magnitudes of the internal volume resistances and the interface resistances in the multilayer system warrant discussion here. The volume thermal resistance of the silicon nitride is approximately 7% of the total thermal resistance measured in the multilayer system in Fig. 2. Therefore, the second term in the middle quantity in (2) results in only a small relative modification of the thermal resistance calculation for the polymer. The silicon nitride thermal conductivity measured here is reduced by the contributions of the resistances at its boundaries with the aluminum overlayer and the silicon substrate. As a result, the use of the silicon nitride thermal conductivity data yields an upper bound for the impact of the thermal resistance of the silicon nitride and its interface with the aluminum overlayer in the more complicated structure used to study the polymer. Therefore, if there are any important boundary resistances influencing the data analysis for the mesa structure in Fig. 2, they are those of the polymer with the overlying silicon nitride or with the underlying aluminum. There are very few data available that provide information about these thermal resistances. One goal of the present study is to provide bounds for their possible magnitudes.

Fig. 4 shows data from the present study for the thermal resistance R_p as a function of the polymer layer thickness. The relative uncertainty estimated for the steady-state measurements reported here is less than 5%. This accounts for the uncertainty in the calibration of the aluminum bridge thermometers, uncertainties in the geometrical dimensions, and the uncertainty of the thermal conductivity of the silicon nitride layer. By assuming that k_{pn} does not vary significantly within the layer thickness, it is possible to extract an upper bound for the thermal boundary resistance at the polymer/silicon substrate interface, $R_b < 10^{-7}$ m^2 K W^{-1}, and to extract the intrinsic thermal conductivity of the polymer $k_{pn} = 0.25 \pm 0.025$ W m^{-1} K^{-1}. This procedure strongly suggests that for the layer thicknesses studied here, the resistances at the polymer boundaries are not significant compared to the polymer vertical volume resistances.

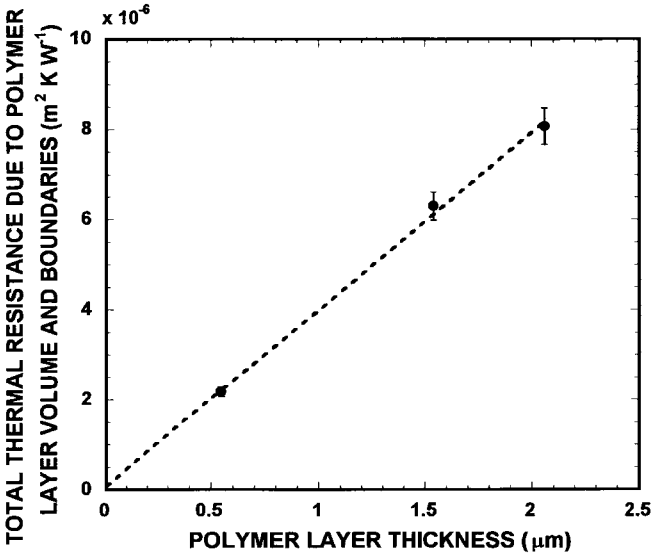

Fig. 4. Total thermal resistance due to the polymer layer volume and the boundaries as a function of layer thickness. The intercept of the line indicates that the sum of the boundary resistances satisfies $0 < R_b < 10^{-7}$ m^2 K W^{-1}.

III. Membrane Lateral Diffusivity Measurement

Few studies have measured the lateral thermal conductivity or diffusivity of polymer layers. Rogers *et al.* [13] measured the lateral thermal diffusivity of polymer films using a technique based on transient gratings. The technique heats a free-standing polymer film using two interfering, picosecond-duration laser pulses and determines the lateral diffusivity from the temporal decay of lateral temperature gradients in the layer. This technique is attractive because no physical contact is required with the sample during the measurement. However, the transient grating technique requires a relatively complicated optical configuration and has a somewhat larger uncertainty than is possible because it measures only the temporal temperature variation and does not use the absolute temperature magnitude. Several studies investigated lateral thermal conduction properties in doped polysilicon

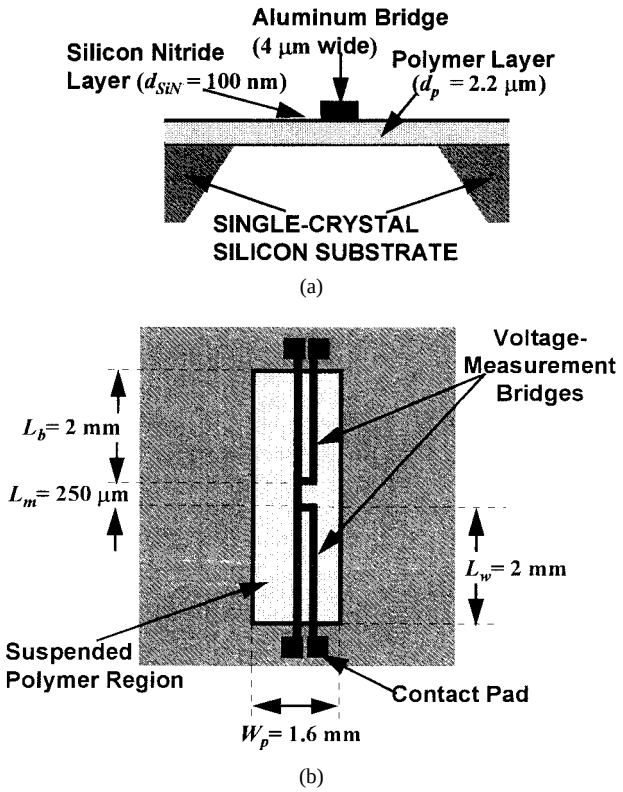

Fig. 5. (a) Cross-sectional and (b) top-view schematics of the microstructure used for measuring the lateral thermal conductivity of the polymer.

layers and in glassy amorphous layers using electrical heating and thermometry in micromachined bridges [32]–[34]. The present work, in this section, describes a similar purely electrical measurement approach that is relatively simple to implement and yields a lower experimental uncertainty. The measurement uses a suspended polymer membrane with a heater/thermometer metal bridge as shown in Fig. 5 to isolate lateral transport. The lateral thermal diffusivity is determined from the normalized in-phase and out-of-phase components of the transient temperature oscillations in the bridge, which is subjected to harmonic Joule heating at ranging frequencies.

The structure in Fig. 5 resembles those used by Völklein [35] for measuring the thermal conductivity and diffusivity of SiO_2/Si_3N_4 composite films. However, the present work uses voltage-measurement bridges connected to the middle portion of the metal bridge, which are far from the contact pads on the membrane edges. This arrangement renders negligible the nonuniform temperature distribution along the middle portion of the metal bridge, simplifying property extraction from the data. The voltage-measurement bridges provide additional heat paths from the middle portion of the bridge to the contact pads. This requires minimization of the measurement errors caused by heat loss due to conduction along the metal bridges.

A. Suspended Membrane Fabrication

The suspended structure is fabricated using silicon etching with a sacrificial silicon dioxide stop layer, an approach that is widely used for making three-dimensional silicon sensors and actuators and is summarized in Fig. 6. First, a silicon dioxide layer of thickness near 3000 Å is grown on both sides of a 4-in silicon wafer using thermal oxidation. Subsequently, a layer of polyamic acid precursor (Du Pont PI 2556, BTDA-ODA-MPD) is spin-coated onto the wafer. A relatively low rotational speed, less than 1000 r/min, is applied during the spin-coating process to yield a thicker polymer film. The polyamic acid film is cured in a nitrogen atmosphere in the same manner as described in Section II. The resulting thickness of the polymer film is 2.2 μm, which is enough to maintain the mechanical strength of the film that will be eventually suspended on the silicon substrate. A silicon nitride layer of thickness near 1000 Å is deposited using PECVD for the same reasons as described in Section II. A 2500-Å film of aluminum is sputtered onto the silicon nitride and patterned using chemical wet etching. A polymer layer of approximately 2-μm thickness is deposited on the sample surface in the same manner as described above. This additional polymer layer protects the aluminum bride from both mechanical damages and chemical corrosions during the processing. The silicon dioxide layer on the back side of the silicon wafer is patterned using hydrofluoric acid (HF) to yield an etch mask for the subsequent silicon back etching. The bulk silicon of the substrate is etched using tetra-methyl-ammonium-hydroxide acid (TMAH). The etching stops at the silicon dioxide layer underlying the polymer film. The silicon-dioxide etch stop layer is removed using an HF solution. Finally, plasma etching removes both the polymer protective layer and the silicon nitride layer covering the polymer surface except the region beneath the metal bridge to complete the whole fabrication process.

B. Experimental Procedure

The measurement procedure adapts the transient 3ω Joule heating and electrical resistance thermometry technique [24]–[27] for the structure in Fig. 5 to provide information about the lateral conductivity of the polymer film. The electrical resistance of the metal bridge is calibrated as a function of temperature on a thermal chuck. The steady-state current applied to the metal bridge during the calibration process must be carefully chosen to avoid a large temperature rise in the suspended membrane, which would unduly complicate the calibration. For this experiment, the maximum current is 0.7 mA and the maximum resulting temperature rise is less than 10 K. Fig. 7 shows a schematic of the experimental setup used for the measurement. Transient Joule heating is sustained in the metal line by means of a harmonic electrical current at angular frequency ω.

The heating frequency used for the measurement is chosen to reduce the experimental uncertainty and simplify data interpretation. The lower bound frequency ensures that the thermal resistance for conduction along the polymer, which increases with the thermal diffusion length along the layer, is very small compared to the thermal resistance for heat loss due to conduction along the metal bridges. The thermometry is performed in the middle portion of the bridge shown in Fig. 8, which is located more than 2 mm from the contact pads at both ends of the bridge and the voltage-measurement bridges. These pads are deposited on the polymer film region supported by the

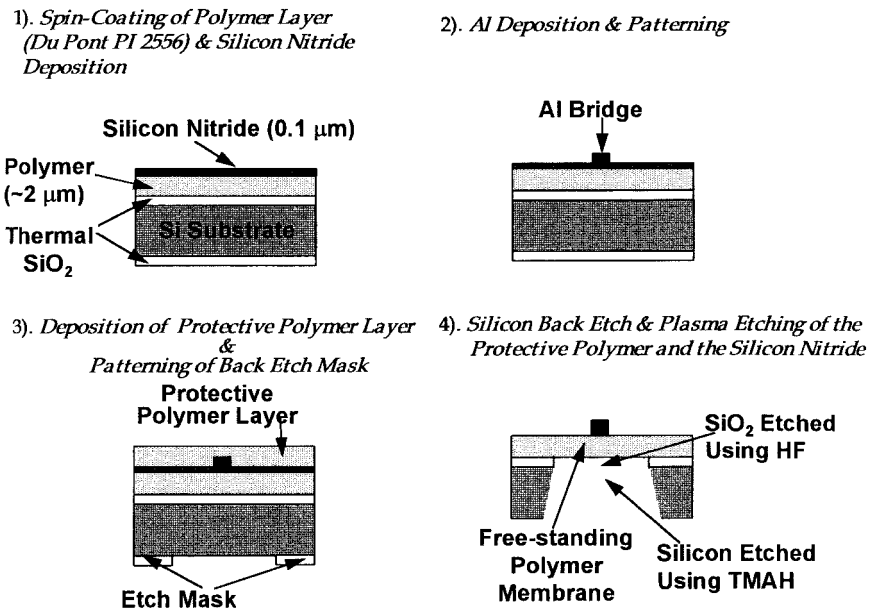

Fig. 6. Microfabrication steps for the structure in Fig. 5.

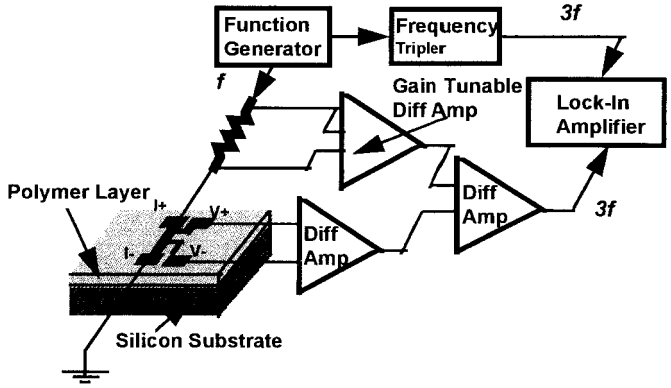

Fig. 7. Experimental apparatus used for measuring the lateral thermal conductivity of the polymer layer. The instrumentation and approach resembles those of Cahill [24].

silicon substrate and therefore have temperatures nearly equal to that of the silicon, which is well modeled as isothermal. This yields a thermal conductance along the metal bridges that can be calculated by assuming a linear temperature drop between the ends of the middle bridge portion and the contact pads

$$G_m = k_m\left(\frac{w_b d_b}{L_b} + \frac{w_w d_w}{L_w}\right) \tag{3}$$

where k_m, w_b, w_m, d_b, d_w, L_b, and L_w are the metal thermal conductivity, the width of the bridge, the width of the voltage-measurement bridge, the thickness of the bridge, the thickness of the voltage-measurement bridge, the distance between the middle portion end and the contact pad along the bridge, and the distance between the middle portion end and the pad along the voltage-measurement bridge, respectively. The apparent thermal resistance offered by the polymer layer can be approximated using a diffusion length form of the solution to the transient heat equation. The thermal diffusion length along the suspended polymer film at heating frequency $f_H = \omega/2\pi$ is given by

$$L_D = \sqrt{\alpha_{pl}/\pi f_H} \tag{4}$$

where α_{pl} is the lateral thermal diffusivity of the polymer film. The thermal conductance from one of the sides of the middle bridge portion to the boundary between the heated and the unheated regions of the suspended polymer film $G_{\rm pH}$ is

$$G_{\rm pH} = \frac{k_{pl} L_m d_p}{L_D} \tag{5}$$

where k_{pl}, L_m, and d_p are the lateral thermal conductivity of the polymer film, the length of the middle portion of the bridge, and the thickness of the polymer film, respectively. The minimum allowable heating frequency $f_{H\,\rm min}$ is estimated by the requirement

$$G_{\rm pH} = 10 G_m \geq G_m \tag{6}$$

which limits the relative experimental error due to the conduction along the metal wires to 10%. Equations (3)–(6) can be combined to yield

$$f_{H\,\rm min} = \frac{\alpha_{pl}}{\pi}\left[\frac{10 k_m}{k_{pl} L_m d_p}\left(\frac{w_b d_b}{L_b} + \frac{w_w d_w}{L_w}\right)\right]^2. \tag{7}$$

Although k_{pl} and α_{pl} are unknown parameters in this measurement, the current work assumes typical values of the thermal conductivity and diffusivity of dielectric materials to estimate the value of $f_{H\,\rm min}$. Using $\alpha_{pl} = 10^{-6}$ m^2 s^{-1}, $k_{pl} = 1$ W m^{-1} K^{-1}, $k_m = 300$ W m^{-1} K^{-1}, $w_b = w_w = 4$ μm, $d_p = 2.2$ μm, $d_b = d_w = 0.3$ μm, $L_m = 250$ μm, and $L_b = L_w = 2$ mm yields $f_{H\,\rm min} = 13.6$ Hz.

When the heating frequency is sufficiently large, the temperature rise in the metal can be influenced by vertical thermal conduction through the thickness of the polymer layer. Since the goal of this measurement is to isolate the lateral conductivity, it is preferable to work at frequencies low enough to

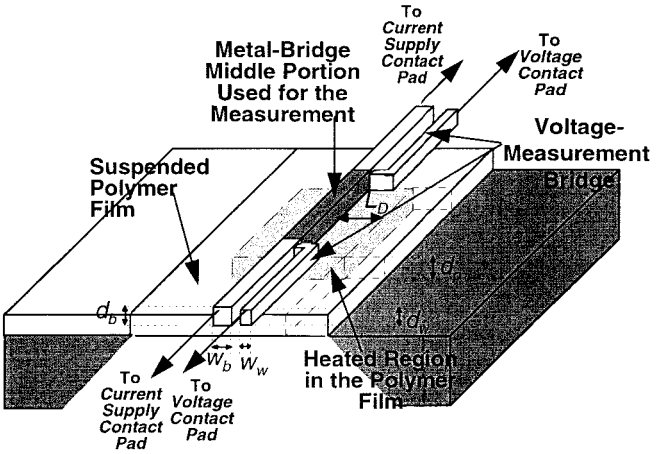

Fig. 8. Physical schematic of the metal bridge and the voltage-measurement bridge deposited on a suspended polymer film.

avoid this complication. Section IV of this paper will document a measurement that simultaneously determines the in-plane and out-of-plane components of the thermal conductivity, for which this restriction is no longer used. For one-dimensional conduction along the membrane to dominate, the following condition must be satisfied:

$$L_D \geq d_p. \tag{8}$$

From (4) and (8), the upper bound of the heating frequency $f_{H\max}$ is given by

$$f_{H\max} = \frac{\alpha_{pl}}{\pi d_p^2}. \tag{9}$$

Using the above values of α_{pl} and d_p yields $f_{H\max} = 66$ kHz. Therefore, the measurements are best confined to heating frequencies between $f_{H\min}$ and $f_{H\max}$.

The measurements are performed in vacuum with a pressure less than 5×10^{-3} torr, where convective heat loss from the sample surface can be neglected. When the temperature rise of the polymer surface ΔT satisfies $\Delta T \ll T_0$, the thermal conductance due to radiation from the heated polymer surface is given by

$$G_R = 8\varepsilon_p \sigma_B T_0^3 L_m L_D \tag{10}$$

where T_0 is the ambient temperature, ε_p is the emissivity of the polymer, and $\sigma_B = 5.67 \times 10^{-8}$, W m^{-2} K^{-4} is the Stefan–Boltzman constant. In the ranges of temperature and heating frequency used in the measurement, $G_R/G_{\rm pH}$ is less than 3×10^{-3} even if the value of ε_p is assumed to be unity. This indicates that the radiative heat loss is negligible.

The in-phase and out-of-phase components of the temperature rise in the bridge with respect to the harmonic heating are obtained from the third harmonic of the voltage drop along the bridge. The temperature-rise response data are analyzed in the frequency domain using complex imbedding and the finite difference method for the structure in Fig. 5. The calculations determine the temperature amplitude and phase in the silicon substrate and account for the possibility of thermal conductivity anisotropy in the polymer, although the frequencies used for the experiment are sufficiently low such

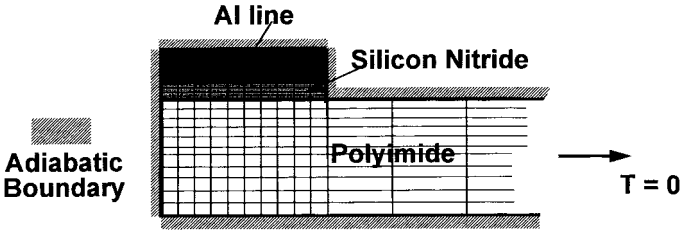

Fig. 9. Configuration and boundary conditions used for studying lateral thermal conduction in the polymer layers using the finite difference method.

that the anisotropy is not important. The analysis also accounts for the isotropic thermal conductivity and the heat capacity of the metal bridge, which are important at the highest heating frequencies. Fig. 9 shows the configuration and the boundary conditions used in the finite difference analysis. The model imposes a uniform volumetric heat density in the aluminum bridge. There are two unknown parameters to be determined using the model: 1) the lateral thermal conductivity k_{pl} and 2) the lateral diffusivity α_{pl}. The diffusivity is related to the thermal conductivity by

$$\alpha_{pl} = k_{pl}/C_v \tag{11}$$

where C_v is the specific heat per unit volume of the polymer layer. The room-temperature value of C_v is assumed to be 1.55 MJ m^{-3} K^{-1} [36], a value which is consistent with recent measurements of the heat capacity of the same films [37]. The frequencies studied here are sufficiently large such that the predicted temperature rises are not significantly influenced by the boundary conditions assumed at the boundaries between the unsupported and supported polymer film regions. However, these frequencies are sufficiently small so that even a 30% error in the value of C_v results in a relative experimental uncertainty less than 5%.

Fig. 10 plots the frequency dependence of both the in-phase and out-of-phase components of the temperature rises at the metal bridge. The value of the lateral thermal conductivity in the polymer is fitted to yield optimal agreement with both the in-phase and out-of-phase data. The best agreement with the data is obtained when the lateral thermal conductivity k_{pl} is about 1.2 W m^{-1} K^{-1}. The estimated relative uncertainty in this measurement is about 15%, which indicates a value for the lateral thermal conductivity of $k_{pl} = 1.2 \pm 0.18$ W m^{-1} K^{-1}. The dominant contributors to the uncertainty include those associated with calibration of the metal temperature sensor and the steady-state component of the temperature rise in the polymer film, which is limited to 20 K in the current measurement. Data for the temperature dependence of the thermal conductivity of polymer film are presented later in this section.

IV. IC Compatible Method

In the previous sections, the thermal conductivities vertical and lateral to polymer films are isolated using relatively complicated micromachining methods, which are not common in IC processing. In contrast, this section develops a complimentary technique which requires only simple patterning

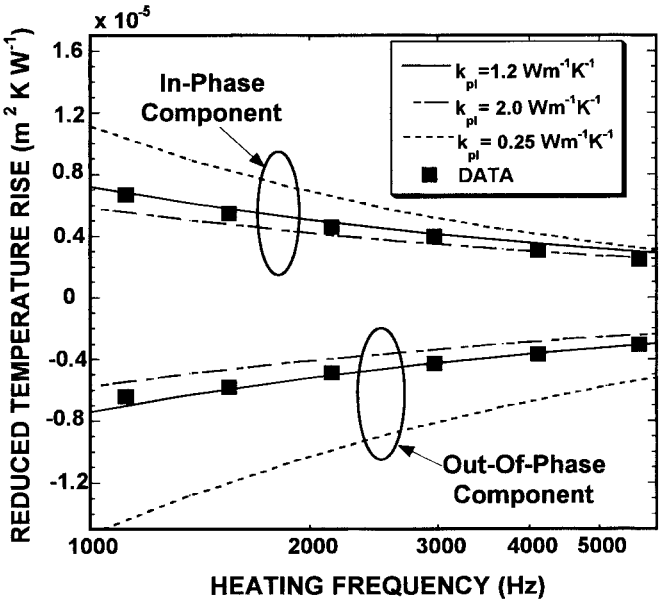

Fig. 10. Prediction and data of the impact of the lateral thermal conductivity of polymer layers on temperature-rise components at the metal bridge for varying values of the heating frequency. The reduced temperature rise is the measured temperature rise (K) divided by both the volumetric heat power density (W m^{-3}) generated at the metal bridge and the metal bridge thickness (m).

of a metal bridge. This measurement yields both the vertical and lateral components of the thermal conductivity using the assumption that the layer is homogeneous.

A. Silicon-Supported Structure Fabrication

The lithography mask used here is designed to yield aluminum bridges of line width varying between 4 and 200 μm on the same die as shown in Fig. 11. Data for bridges of varying width enables one to extract both the vertical and lateral thermal conductivities of the same polymer film sample. Polymer layers of thickness between 0.5 and 2.5 μm are deposited and cured on a bare silicon wafer coated with the organic adhesion-promoter in the same manner as described in Section II-A. The polymer layer is subsequently covered with a 1000-Å-thick PECVD silicon nitride layer. An aluminum layer of thickness 2500 Å is sputtered and patterned on the silicon nitride layer. Finally, the silicon nitride layer covering the polymer is removed except from the region beneath the metal bridge using plasma etching.

B. Experimental Procedure

The transient Joule heating and electrical resistance thermometry described in Section III are employed here to examine the impact of both the vertical and lateral thermal conduction in the polymer for aluminum bridges of varying width. A harmonic current generates heating in the bridges. The electrical resistance of each bridge is calibrated such that the bridge serves as a thermometer as well as a heater. The transient temperature-rise responses at the bridge are measured to extract thermal conductivities of the polymer films.

At first, the measurement is performed for the metal bridge of width 200 μm, which is more than two orders of magnitude

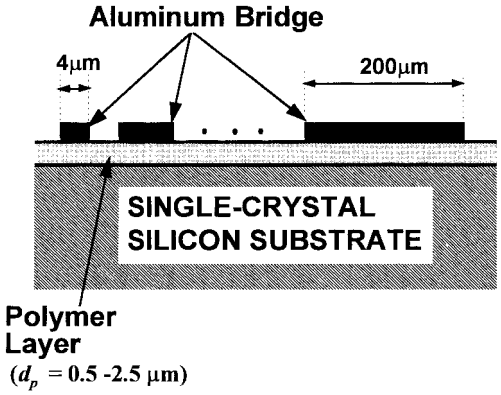

Fig. 11. Cross-sectional schematic of the microstructure used for measuring both the vertical and the lateral thermal conductivities in the same polymer film. Metal bridges of line width varying between 4 and 200 μm are deposited on the same silicon substrate.

larger than the polymer film thickness. When the bridge width is much larger than the polymer thickness, the thermal conduction is nearly one dimensional in the direction normal to the film, and the vertical conductivity has a dominant influence on the temperature rise. Compared to the perfectly one-dimensional case, the error resulting from the use of this structure is no more than 3% throughout the frequency range used in the measurement, even if the lateral conductivity is one order of magnitude larger than the vertical conductivity. Fig. 12 shows temperature-rise response data for the metal bridges of width 200 μm deposited on a polymer film of thickness 2.5 μm together with data obtained from subsequent measurements for the metal bridge of width 4 μm on the same film. Using the finite-difference method described in the previous section, theoretical curves are fitted to the data for extracting the vertical thermal conductivity of the film first. The calculation yields the best agreement with the data when the vertical thermal conductivity k_{pn} is approximately 0.25 W m^{-1} K^{-1}. The temperature-rise signal from the bridge of width 200 μm is highly sensitive to the vertical thermal conductivity at frequencies lower than 3 kHz and is not significantly influenced by the specific heat of the films. The large sensitivity of the measurement yields relatively small experimental uncertainties, which are estimated to be less than 8% accounting for the error resulting from the imperfect one-dimensionality in the current structure.

The lateral thermal conductivity is extracted using the data for the narrow bridge of width 4 μm, which are sensitive to both the vertical and lateral thermal conductivities. Using $k_{pn} = 0.25$ W m^{-1} K^{-1} obtained above, the lateral thermal conductivity is extracted by fitting the calculated curve to the experimental data in Fig. 12. The best agreement is obtained when the lateral thermal conductivity k_{pl} is about 1.5 W m^{-1} K^{-1}. The specific heat of the polymer films is also assumed to be 1.55 MJ K^{-1} m^{-3} here. The sensitivity of the measurement to the lateral conductivity increases with decreasing values of the ratio of the bridge width to the polymer thickness. This means that the experimental uncertainty decreases with decreasing bridge width. The current structure still yields an experimental uncertainty as large as 30%.

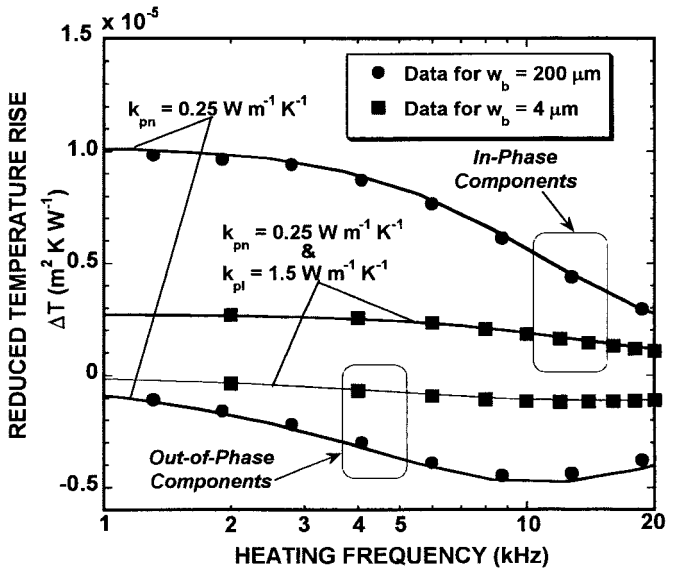

Fig. 12. Prediction and data for the impact of the vertical and the lateral thermal conductivity of polymer layers on temperature-rise components of the metal bridge for varying values of the heating frequency. A significant temperature reduction is observed for the narrow metal bridge due to the lateral heat spreading in the film. This spreading is aided by the larger lateral conductivity.

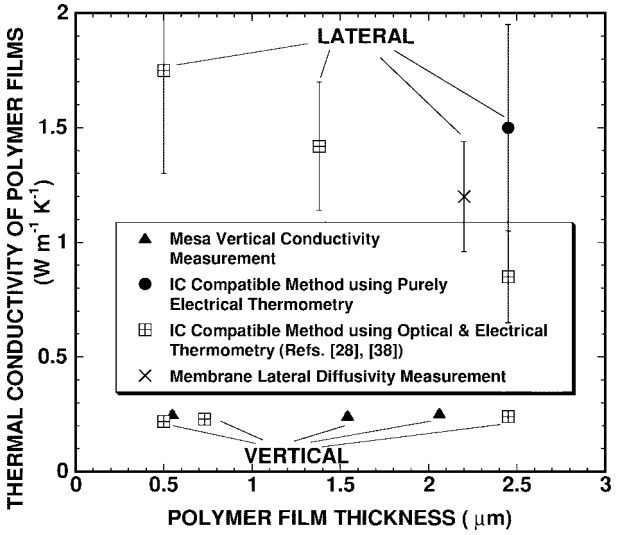

Fig. 13. Thermal conductivity vertical and lateral to polymer layers as a function of layer thickness.

V. Results and Discussion

A. Film Thickness Dependence of the Conductivities

Fig. 13 plots data for the effective vertical thermal conductivity, which is defined by $k^e_{pn} \equiv d_p/R_p$, and the lateral thermal conductivity for varying polymer film thickness. The data show that polyimide films deposited using spin-coating exhibit significant anisotropy in thermal conductivity, which favors lateral conduction by a factor between four and eight. Fig. 13 also includes data obtained for measurements performed at different film thicknesses and different locations on the same sample using another method, which combines Joule heating and laser-reflectance thermometry at frequencies up to 100 kHz [28], [38]. The data obtained using the present method and the method using optical thermometry agree within the experimental uncertainty. Considering the uncertainty, we observe no thickness dependence of the thermal conductivity anisotropy within the range of thicknesses shown.

Thermal conductivity anisotropy has been studied for uniaxially drawn bulk polymers and the data are summarized elsewhere [39]. When those polymers are uniaxially stretched with a draw force, the chain molecules tend to align along the draw direction. The molecular alignment is augmented with increasing draw ratio. Consequently, the polymers exhibit large thermal conductivity anisotropy and the conductivity along the draw direction to that in the perpendicular direction increases with the draw ratio. This phenomenon can be very approximately interpreted using the kinetic theory for heat conduction in solids by phonons, which are the quanta of atomic vibrational energy. The thermal conductivity is [40]

$$k = \tfrac{1}{3}\, C_{\rm ph} v l \qquad (12)$$

where $C_{\rm ph}$ is the phonon specific heat, v is the acoustic velocity, and l is the phonon mean free path. In highly disordered materials, the application of (12) is made questionable by the fact that the phonon mean free path is comparable to the phonon wavelength, which renders an atomistic theory far more appropriate. However, (12) can be used to interpret the mechanisms responsible for the anisotropy in the layer. The overlap of the carbon π-orbitals along the covalently bonded chain yields larger elastic constants for vibrations propagating along the chains than for those propagating between neighboring chains. Vibrations propagating between neighboring chains have velocity governed by the lower intermolecular force constants, which are governed by the van der Waals interaction. Although conduction between neighboring chains closely resembles that in amorphous glasses, for which the mean free path is comparable to the interatomic separation, the mean free path along chains could be higher due to the strong interatomic coupling. These arguments indicate that both the velocity and the mean free path may be higher along chains than between neighboring chains. Therefore, chain alignment in the film plane enhanced the lateral thermal conductivity. A more quantitative description of the anisotropy needs to consider the statistical distribution of chain orientation in a layer, which can be examined using X-ray diffraction [41], [42] and the polarized infrared absorption spectroscopy [43].

B. Temperature Dependence

We report the temperature dependence of the thermal conductivity anisotropy of a polymer film of thickness 2.25 μm using the micromesa and the membrane techniques. The sample is placed in a cryostat and the ambient temperature was varied using a thermal controller. The measurement analysis requires data for the thermal conductivities and heat capacities of silicon, aluminum, and silicon nitride, and for the heat capacity of the polymer film as functions of temperature. The current work uses thermal conductivity values obtained from published literature [44]–[47]. The transient method requires

TABLE I
SUMMARY OF EXPERIMENTAL TECHNIQUES DEVELOPED IN THE CURRENT WORK

Technique	Measured Conductivity	Experimental Structure	Advantages	Disadvantages	Experimental Uncertainties
1. Mesa Vertical Conductivity Measurement	Vertical Thermal Conductivity k_{pn}	Metal/Polymer/ Metal Stack	• Simple Data Analysis • High Accuracy	• Precise Alignment of Patters during the Fabrication	+/- 5 %
2. Membrane Lateral Diffusivity Measurement	Lateral Thermal Conductivity k_{pl}	Suspended Polymer Film	• Accurate Data Extraction • Low Radiative Heat Loss	• No Simple Analytical Solution Form Available for the Data Extraction	+/- 15 %
3. IC Compatible Method	Vertical & Lateral Thermal Conductivity k_{pn} & k_{pl}	Polymer Film Supported on Silicon	• Simple Fabrication (IC Fabrication Compatible) • Simple Equipment	• Tedious Data Extraction • Large Experimental Uncertainties	k_{pn} +/- 8 % k_{pl} +/- 30 %

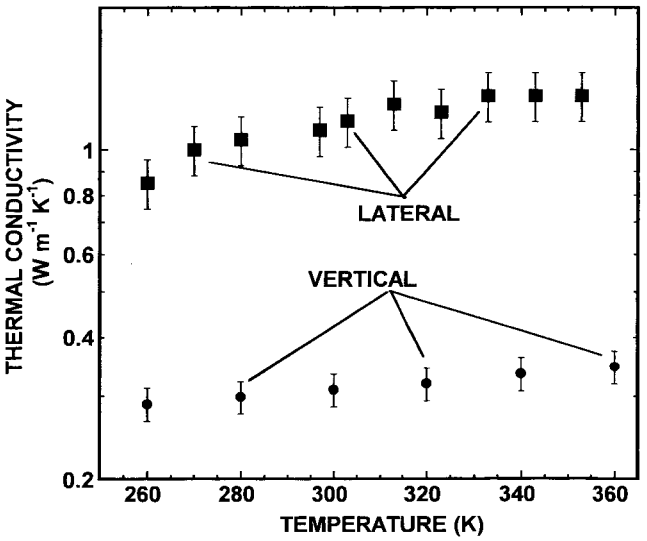

Fig. 14. Temperature dependence of thermal conductivity anisotropy of a polymer film of thickness 2.25 μm.

the heat capacity data for the polymer film. The capacity of the film is independently measured by capturing a transient temperature-rise response at a test structure similar to the micromesa. The details of the measurement are described elsewhere [37]. Fig. 14 shows the vertical and lateral thermal conductivities at temperatures varying between 260 and 360 K. Further studies on temperature dependence of both the specific heat and the acoustic velocity along the in-plane and the out-of-plane directions are needed to interpret these data.

VI. SUMMARY AND CONCLUSIONS

This manuscript describes measurements of the vertical and the lateral thermal conductivities in polymer layers using three independent techniques. Table I summarizes these techniques and shows both the advantages and disadvantages associated with each method. The data are obtained at room temperature using these independent techniques and are consistent, which helps to validate the relatively straightforward IC compatible approach. For the layer thicknesses studied here, the effective vertical thermal conductivity appears to be relatively homogeneous and not significantly reduced by resistances at the layer boundaries. The data reported here indicate that the lateral thermal conductivity is larger by a factor of six than the effective vertical thermal conductivity for film thicknesses between 0.5 and 2.5 μm. Since boundary resistances do not significantly reduce the vertical thermal conductivity, the anisotropy would have to occur within the volume of the polymer and might be explained by the partial alignment of molecular chains. The anisotropy is particularly important for MEMS actuators that are based on polymer films, in which lateral thermal conduction dominates the response time. The anisotropy can be expected to decrease the heat-diffusion time by a factor approximately equal to the square of the anisotropy factor, according to the heat-diffusion equation, compared to the time constant calculated using the bulk thermal diffusivity.

The temperature dependence of the thermal conductivities in vertical and lateral directions of polymer films is studied using the techniques developed here. The results show that the thermal energy propagation efficiency becomes larger in the both directions as the background temperature of the films increases. The physics of the anisotropic thermal conduction along and perpendicular to polymer chains needs to be fully understood to explain the temperature behaviors of the thermal conductivity. A future study will characterize the molecular-level structures of the polymer films and compare the molecular orientation with the data obtained in the current study.

REFERENCES

[1] T. Ebefors, E. Kalvesten, and G. Stemme, "Dynamic actuation of polyimide V-groove joints by electrical heating," *Sens. Actuators A*, vol. A67, pp. 199–204, 1998.

[2] J. W. Suh, S. F. Glander, R. B. Darling, C. W. Storment, and G. T. A. Kovacs, "Organic thermal and electrostatic ciliary microactuator array for object manipulation," *Sens. Actuators A*, vol. A58, pp. 51–60, 1997.
[3] K. R. Carter, H. J. Cha, R. A. Dipietro, C. J. Hawker, J. L. Hedrick, J. W. Labadie, J. E. McGrath, T. P. Russell, M. I. Sanchez, S. A. Swanson, W. Volksen, and D. Y. Yoon, "Polyimide nanofoams for low dielectric applications," in *Materials Rec. Soc. Symp. Proc.*, 1995, vol. 381, pp. 79–91.
[4] R. J. Gutmann, T. P. Chow, D. J. Douquette, T.-M. Lu, J. F. McDonald, and S. P. Murarka, "Low dielectric constant polymers for on-chip interlevel dielectrics with copper metallization," in *Materials Rec. Soc. Symp. Proc.*, 1995, vol. 381, pp. 177–195.
[5] Y. K. Lee, S. P. Murarka, S.-P. Jeng, and B. Auman, "Investigation of the low dielectric constant fluorinated polyimide for use as the interlayer dielectric in ULSI," in *Materials Rec. Soc. Symp. Proc.*, 1995, vol. 381, pp. 31–43.
[6] P. E. Burrows, G. Gu, V. Bulovic, Z. Shen, S. R. Forrest, and M. E. Thompson, "Achieving full-color organic light-emitting devices for lightweight, flat-panel displays," *IEEE Trans. Electron Devices*, vol. 44, pp. 1188–1203, 1997.
[7] L. Lin and S. A. Bidstrup, "Processing effects on optical anisotropy in spin-coated polyimide films," *J. Appl. Polym. Sci.*, vol. 49, pp. 1277–1289, 1993.
[8] S. Herminghaus, D. Boese, D. Y. Yoon, and B. A. Smith, "Large anisotropy in optical properties of thin polyimide films of poly(*p*-phenylene biphenyltetracarboximide)," *Appl. Phys. Lett.*, vol. 59, pp. 1043–1045, 1991.
[9] D. Boese, S. Herminghaus, D. Y. Yoon, J. D. Swalen, and J. F. Rabolt, "Stiff polyimides: Chain orientation and anisotropy of the optical and dielectric properties of thin films," in *Materials Rec. Soc. Symp. Proc.*, 1991, vol. 227, pp. 379–386.
[10] P. S. Ho, T. W. Poon, and J. Leu, "Molecular structure and thermal/mechanical properties of polymer thin films," *J. Phys. Chem. Solids*, vol. 55, pp. 1115–24, 1994.
[11] J. Leu, S. Kang, H. C. Liou, and P. S. Ho, "The effect of curing on the thermomechanical properties of BPDA-PDA polyimide thin films," in *Electronic Packaging Materials Science VII, Materials Res. Soc.*, 1994, pp. 283–8.
[12] T. W. Poon, J. Leu, Y. S. Kang, H. C. Liu, and P. S. Ho, "Morphological effects on the materials properties of polyimides," in *Electronic Packaging Materials Science VII, Materials Res. Soc.*, 1994, pp. 333–44.
[13] J. A. Rogers, Y. Yang, and A. Nelson, "Elastic modulus and in-plane thermal diffusivity measurements in thin polyimide films using symmetry-selective real-time impulsive stimulated thermal scattering," *Appl. Phys. A*, vol. 58, pp. 523–534, 1994.
[14] C. L. Choy, S. P. Wong, and K. Young, "Model calculation of the thermal conductivity of polymer crystals," *J. Polymer Sci.: Polymer Phys. Edition*, vol. 23, pp. 1495–1504, 1985.
[15] D. T. Morelli, J. Hermans, M. Sakamoto, and C. Uher, "Anisotropic heat conduction in diacetylenes," *Phys. Rev. Lett.*, vol. 57, pp. 869–872, 1986.
[16] K. E. Goodson and M. I. Flik, "Solid layer thermal-conductivity measurement techniques," *Appl. Mech. Rev.*, vol. 47, pp. 101–112, 1994.
[17] D. G. Cahill, 1997, "Heat transport in dielectric thin films and at solid-solid interfaces," *Microscale Thermophys. Eng.*, vol. 1, pp. 85–109, 1997.
[18] E. T. Swartz and R. O. Pohl, "Thermal resistance at interfaces," *Appl. Phys. Lett.*, vol. 51, pp. 2200–2202, 1987.
[19] K. E. Goodson, M. I. Flik, L. T. Su, and D. A. Antoniadis, "Prediction and measurement of the thermal conductivity of amorphous dielectric layers," *J. Heat Transfer*, vol. 116, pp. 317–324, 1994.
[20] M. B. Kleiner, S. A. Kühn, and W. Weber, "Thermal conductivity measurements of thin silicon dioxide films in integrated circuits," *IEEE Trans. Electron Devices*, vol. 43, pp. 1602–1609, 1996.
[21] F. Völklein and E. Kessler, "A method for the measurement of thermal conductivity, thermal diffusivity, and other transport coefficients of thin films," *Phys. Stat. Sol. A*, vol. 81, pp. 585–596, 1984.
[22] M. Okuda and S. Ohkubo, "A novel method for measuring the thermal conductivity of submicrometer thick dielectric films," *Thin Solid Films*, vol. 213, pp. 176–181, 1992.
[23] O. W. Käding, H. Shurk, and K. E. Goodson, "Thermal conduction in metallized silicon-dioxide layers on silicon," *Appl. Phys. Lett.*, vol. 65, pp. 1629–1631, 1994.
[24] D. G. Cahill, "Thermal conductivity measurement from 30 to 750 K: The 3ω method," *Rev. Sci. Instrum.*, vol. 61, pp. 802–808, 1990.
[25] D. G. Cahill, M. Katiyar, and J. R. Abelson, "Thermal conductivity of a-Si:H thin films," *Phys. Rev. B*, vol. 50, pp. 6077–6081, 1994.
[26] S. M. Lee, D. G. Cahill, and T. H. Allen, "Thermal conductivity of sputtered oxide films," *Phys. Rev. B*, vol. 52, pp. 253–257, 1995.
[27] S. M. Lee and D. G. Cahill, "Heat transport in thin dielectric films," *J. Appl. Phys.*, vol. 81, pp. 2590–2595, 1997.
[28] Y. S. Ju, K. Kurabayashi, and K. E. Goodson, "Thermal characterization of IC passivation layers using joule heating and optical thermometry," *Microscale Thermophys. Eng.*, vol. 2, pp. 101–110, 1998.
[29] H. G. Kilian and M. Pietralla, "Anisotropy of thermal diffusivity of uniaxial stretched polyethylenes," *Polymer*, vol. 19, pp. 664–672, 1978.
[30] K. Blum, H. G. Kilian, and M. Pietralla, "A method for measuring the anisotropy ratio of the thermal conductivity of anisotropic solids," *J. Phys. Part E: Sci. Instrum.*, vol. 16, pp. 807–812, 1983.
[31] J. Rantala, "A measurement method for the determination of the anisotropy ratio of thermal conductivity of plastic foils," *Rev. Sci. Instrum.*, vol. 63, pp. 5472–5474, 1992.
[32] F. Völklein and H. Baltes, "A microstructure for measurement of thermal conductivity of polysilicon thin films," *IEEE J. Microelectromech. Syst.*, vol. 1, pp. 193–196, 1992.
[33] O. M. Paul, J. Korvink, and H. Baltes, "Determination of the thermal conductivity of CMOS IC polysilicon," *Sens. Actuators A*, vol. A41-42, pp. 161–164, 1994.
[34] X. Zhang and C. P. Grigoropoulos, "Thermal conductivity and diffusivity of free-standing silicon nitride thin films," *Rev. Sci. Instrum.*, vol. 66, pp. 115–1120, 1995.
[35] F. Völklein, "Thermal conductivity and diffusivity of a thin film SiO_2-Si_3N_4 sandwich system," *Thin Solid Films*, vol. 188, pp. 27–33, 1990.
[36] Du Pont PYRALIN® PI 2556 Material Data Sheet, Du Pont Co., Wilmington, DE.
[37] K. Kurabayashi, "Thermal transport properties of organic films for advanced VLSI systems," Ph.D. dissertation, Stanford Univ., Stanford, CA, 1998.
[38] Y. S. Ju, K. Kurabayashi, and K. E. Goodson, "Thermal characterization of anisotropic thin dielectric films using harmonic Joule heating," *Thin Solid Films*, vol. 339, pp. 160–164, 1999.
[39] C. L. Choy, "Thermal conductivity of polymers," *Polymer*, vol. 18, pp. 984–1004, 1977.
[40] J. M. Ziman, *Electrons and Phonons.* Oxford, U.K.: Oxford Univ. Press, 1960, pp. 221–223.
[41] N. Takahashi, D. Y. Yoon, and W. Parrish, "Molecular order in condensed states of semiflexible polyamic acid and polyimide," *Macromolecules*, vol. 17, pp. 2583–2588, 1984.
[42] T. P. Russel and H. R. Brown, "X-ray studies on the deformation of an aromatic polyimide," *J. Polym. Sci. B, Polym. Phys.*, vol. 25, pp. 1129–1148, 1987.
[43] K. Sakamoto, R. Arafune, N. Ito, and S. Ushioda, "Determination of molecular orientation of very thin rubbed and unrubbed polyimide films," *J. Appl. Phys.*, vol. 80, pp. 431–439, 1996.
[44] Y. S. Touloukian and E. H. Buyco, "Thermal conductivity: Nonmetallic solids," in *Thermophysical Properties of Matter.* New York: IFI/Plenum, vol. 2, pp. 1–9, 1970.
[45] ——, "Specific heat: Nonmetallic solids," in *Thermophysical Properties of Matter.* New York: IFI/Plenum, vol. 5, pp. 1–5, 1970.
[46] ——, "Thermal conductivity: Metallic elements and alloys," in *Thermophysical Properties of Matter.* New York: IFI/Plenum, vol. 1, pp. 1–9, 1970.
[47] Y. S. Touloukian and E. H. Buyco, "Specific heat metallic elements and alloys," in *Thermophysical Properties of Matter.* New York: IFI/Plenum, vol. 4, pp. 1–5, 1970.

Katsuo Kurabayashi received the B.S. degree in precision machinery engineering from the University of Tokyo, Japan, in 1992 and the M.S. and Ph.D. degrees in materials science and engineering from Stanford University, Stanford, CA, in 1994 and 1998, respectively.

He is a Physical Science Research Associate with the Mechanical Engineering Department, Stanford University. His current research interest is in development of microfluidic MEMS devices for cooling IC chips and the use of MEMS structures for thermal property analysis of thin films.

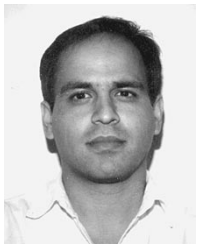

Mehdi Asheghi received the B.S. degree from the Mechanical Engineering Department at Sharif University of Technology, Iran, in 1991 and the M.S. degree in mechanical engineering from California State University Long Beach in 1993. He is a Ph.D. candidate in mechanical engineering at Stanford University, Stanford, CA. His Ph.D. studies include investigation on thermal properties of nearly pure and doped thin silicon films.

Maxat Touzelbaev received the B.S. degree with the red diploma award from the Department of Mechanics and Applied Mathematics at Kazakh State University, Kazakhstan, in 1992 and the M.S. degree in mechanical engineering from the University of Arkansas, Fayetteville, in 1994. He is a Ph.D. candidate in mechanical engineering at Stanford University, Stanford, CA. His Ph.D. studies included investigation on thermal properties of novel superlattice thin films using photothermal reflectance methods.

He spent the autumn of 1996 and 1997 with the Materials Research Group, Daimler-Benz AG, Ulm, Germany.

Kenneth E. Goodson received the B.S., M.S., and Ph.D. degrees in mechanical engineering from the Massachusetts Institute of Technology, Cambridge, in 1989, 1991, and 1993, respectively.

He joined Stanford University, Stanford, CA, in 1994, where he is an Assistant Professor with the Thermosciences Division of the Mechanical Engineering Department. He spent 16 months with Daimler-Benz AG, Germany, working with the Materials Research Group on the thermal design of power circuits for vehicles. At Stanford, he mentors 11 doctoral candidates and post-doctoral associates who are investigating the thermal engineering of electronic microstructures. He is author or coauthor of more than 35 archival journal articles and three book chapters. He is a Daimler-Benz CMG Research Advisor and a Texas Instruments FMA Program Advisor. In Spring 1996, he was a JSPS Visiting Professor at the Tokyo Institute of Technology.

Dr. Goodson has received the ONR Young Investigator Award and the NSF CAREER Award.